Effects of hydrostatic pressure on free and bound exciton states in silver bromide

1990 J. Phys.: Condens. Matter 2 919

(http://iopscience.iop.org/0953-8984/2/4/012)

J. Phys.: Condens. Matter 2 (1990) 919–929. Printed in the UK

Effects of hydrostatic pressure on free and bound exciton states in silver bromide

W Wassmuth, H Stolz and W von der Osten
Fachbereich Physik, Universität-GH Paderborn, D-4790 Paderborn, Federal Republic of Germany

Received 18 July 1989

Abstract. In AgBr at low temperature, resonant Raman scattering is employed to investigate the $\Gamma_6^+ \otimes L_{4,5}^-$ indirect free exciton state under hydrostatic pressure up to 0.7 GPa. From the pressure dependence of resonance behaviour and Raman energy shifts, the deformation potential constant of the exciton edge and mode Grüneisen parameters of various phonons involved in exciton relaxation are obtained simultaneously. Also, the effect of pressure on several bound exciton states is studied by luminescence. Donor-bound excitons of type (D^0, X) with localisation energies $E_1 = 6$ to 8 meV show a negative pressure shift ($dE/dP = -15.1$ meV GPa^{-1}) completely parallel to the free exciton gap proving their effective-mass nature with wavefunctions identical to those of the free exciton. Similarly, the iodine-bound exciton state ($E_1 = 43$ meV) is found to derive mainly from the L-point valence band states with only minor contributions from Γ. Different contributions to the pressure-induced change in lattice relaxation occurring in this case are determined and discussed.

1. Introduction

Hydrostatic pressure is well established as a tool with which to study the effect of change in unit cell volume on electronic states in crystals. To investigate the pressure dependence of the indirect exciton state in the silver halides AgCl and AgBr, in early work (Brothers and Lynch 1969) conventional absorption measurements were used to probe the pressure effects. One difficulty in performing a precise analysis of data is to determine the absorption threshold energies of the indirect exciton as a function of pressure from the energy dependence of the absorption constant which deviates considerably from the expected square root behaviour (see e.g. Sliwczuk *et al* 1984). In addition, the pressure does not only affect the electronic but also the vibrational energies. Since the exciton in silver halides has indirect character, i.e. exciton transitions are accomplished by momentum-conserving phonons, a prerequisite for determining the volume dependence of the exciton gap energy from the absorption is knowledge of the volume (or pressure) dependence of the corresponding phonon energies.

A suitable optical technique to obtain, in silver halides, the necessary information on the pressure-induced change of electronic and vibrational energies simultaneously is resonant Raman scattering excited in resonance with the indirect exciton absorption (Windscheif and von der Osten 1980). We have employed this method on AgBr and in this paper communicate the results obtained. In addition, we investigated a number of bound exciton states under pressure in this material by studying recombination

0953-8984/90/040919 + 11 $03.50

luminescence from them. These experiments yield information on the band states from which the bound exciton states derive, as well as on the pressure dependence of the relevant electron–lattice interaction.

2. Experimental technique

The resonant Raman scattering and luminescence measurements were performed with an experimental set-up consisting of a tunable dye laser as excitation source and a 1 m double monochromator and photon counting equipment for signal detection. The samples were grown by the Bridgman technique at the University of North Carolina or in our Crystal Growing Facility. They were cut and carefully polished as described earlier (see e.g. Windscheif and von der Osten 1980). The samples were unoriented with a typical size of $4 \times 3 \times 3$ mm^3.

The pressure experiments were performed with the sample built in a four-window optical high pressure cell (Fitchen 1963) allowing a 90° scattering geometry. The cell was clamped to a continuous helium flow cooling unit rendering achievable variable temperatures down to 7 K. The temperature was measured by a sensor built into one of the window openings. As the pressure medium, we used helium gas compressed by a gas-compressor system and a pressure amplifier connected to the optical cell by a high pressure tube. At low temperatures, the pressure inside the cell was determined by the helium-gas pressure before solidification by using the equation of state for solid ^{4}He (Dugdale 1958). The maximum pressure reached was 0.7 GPa. The experimental uncertainty in pressure determination is about 1%. For measurements at normal pressure, a variable-temperature continuous helium flow cryostat was used.

To control the hydrostatic pressure conditions, we used the zero-phonon line of the iodine-bound exciton (line I^{ZP} in figure 5—see later). By electron–hole exchange interaction, this line is split into a symmetry-allowed A component and a forbidden B component (Czaja and Baldereschi 1979), which are observed under sufficiently high spectral resolution (not shown). The forbidden B component becomes optically allowed by effects lowering the crystal symmetry, its intensity thus being sensitive to uniaxial stress components. Under non-hydrostatic pressure conditions, which we tried to avoid, we accordingly observed an increase of the B-line intensity relative to that of the A line.

3. Experimental results and analysis

3.1. Pressure dependence of the indirect free exciton state

In AgBr at low temperature, for excitation at and above the indirect exciton absorption threshold (energy $E^i_{ax} = 2.6927$ eV), Raman scattering in resonance with the free exciton state takes place with assistance of momentum-conserving L-point phonons. Beside the most intense 2TO(L) scattering, additional processes are observed due to intraband exciton scattering involving various Γ-point phonons and intervalley scattering between non-equivalent L points mediated by X-point phonons (for a comprehensive discussion of these processes see e.g. von der Osten 1984). The investigation of these processes in samples under hydrostatic pressure enables one to obtain the pressure effects on the electronic and phonon energies simultaneously and to determine their contributions to the energy shift of the exciton absorption threshold separately.

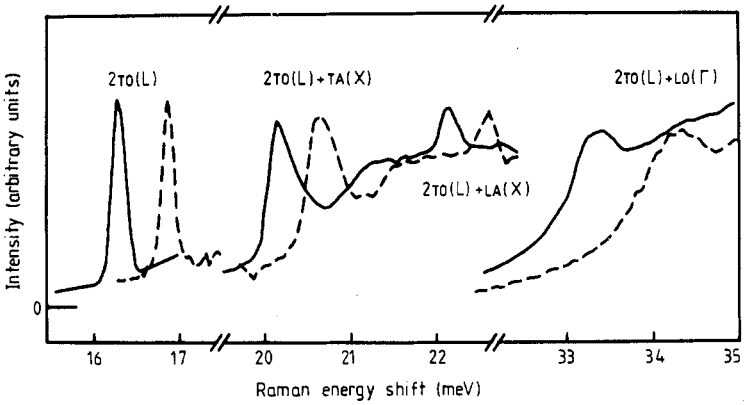

Figure 1. Resonant Raman scattering spectra in AgBr at $P = 0$ GPa (full curves) and $P = 0.573$ GPa (broken curve) at $T = 7$ K. The excitation energies ε relative to the exciton absorption threshold are: $\varepsilon = 3.1$ meV for 2TO(L), $\varepsilon = 7.7$ meV for 2TO(L) + TA(X) and 2TO(L) + LA(X), $\varepsilon = 20.6$ meV for 2TO(L) + LO(Γ).

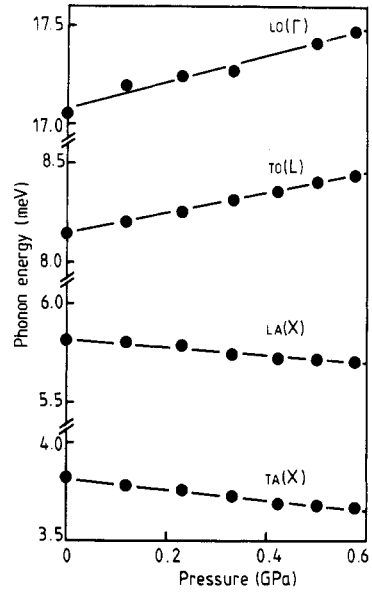

Figure 2. Pressure dependence of phonon energies for various acoustic and optical phonons in AgBr at 7 K obtained from resonant Raman scattering.

3.1.1. Phonons and mode Grüneisen parameters. In figure 1 examples of Raman scattering lines investigated in this work are shown. From the Raman energy shifts (peak position relative to incident laser photon energy) the pressure dependence of the various phonon energies is obtained and represented in figure 2. The data are summarised in table 1 together with the calculated mode Grüneisen parameters defined by

$$\gamma = B_T \Omega_0^{-1} \, \mathrm{d}\Omega/\mathrm{d}P \tag{1}$$

where Ω is the phonon frequency (Ω_0: phonon frequency at normal pressure) and $B_T =$

Table 1. Phonon energies $\hbar\Omega_0$ at normal pressure, pressure shift of phonon energies $d(\hbar\Omega)/dP$ and mode Grüneisen parameters γ at $T = 7$ K.

	$\hbar\Omega_0$	$d(\hbar\Omega)/dP$	γ
TO(L)	8.2 meV	+0.51 meV GPa^{-1}	$+2.8 \pm 0.4$
LO(Γ)	17.1 meV	+0.66 meV GPa^{-1}	$+1.7 \pm 0.8$
LA(X)	5.8 meV	−0.21 meV GPa^{-1}	-1.6 ± 0.8
TA(X)	3.8 meV	−0.27 meV GPa^{-1}	-3.2 ± 0.8

$-V_0\,dP/dV$) is the isothermal bulk modulus which for AgBr at low temperature (4.2 K) was taken as $B_T = 45.3 \pm 0.5$ GPa (Marklund *et al* 1969). Inspecting the data, two distinctly different behaviours are recognised. The two optical phonons (TO(L), LO(Γ)) exhibit a positive pressure coefficient caused by the increase in strength of repelling forces with decreasing volume. In contrast, the acoustic X phonons are lowered in energy showing some kind of 'soft-mode' behaviour. This suggests an increasing instability of the crystal lattice with pressure which, from the eigenvectors of these modes, involves displacements along ⟨100⟩ crystal directions. An extrapolation of the pressure dependence in figure 2 to zero energy (thereby neglecting any deviation from linearity) gives a value of about 10 GPa for a possible structural phase transition to occur. In fact, for AgBr (at room temperature) at $P = 8.4$ GPa, a discontinuous shift of the band edge was observed earlier (Slykhouse and Drickamer 1958), which had been interpreted as being caused by a structural change. From x-ray diffraction it later proved to be due to a transition from the NaCl structure to a high pressure phase with (hexagonal) HgS structure (Schock and Jamieson 1969). This structure may be considered a perturbed NaCl structure with the transition accomplished essentially by a distortion of the cation/anion chains along ⟨100⟩ supposedly initiated by these X-point phonons.

3.1.2. Indirect exciton gap. Figure 3 displays excitation spectra of the 2TO(L) scattering line in figure 1 at different pressures. We found the scattered intensity to decrease slightly at higher pressure. The (normalised) integrated intensity is plotted versus laser photon energy E_L with the actual position of the 2TO(L) line shifted by $2\hbar\Omega^{TO(L)}$ to lower energies corresponding to the two phonons involved. The full lines are fits to the experimental data where we applied an analysis that includes intra- and intervalley exciton scattering by various zone centre and off-centre phonons and that had been extensively discussed in a previous publication (Windscheif and von der Osten 1980). In the model used, the 2TO(L) scattered intensity as function of exciton kinetic energy ε may be written as

$$I^{2TO(L)}(\varepsilon) \sim \varepsilon^{1/2}/[C_0 + C_{ac}\varepsilon + C_{iv}(2\varepsilon - \hbar\Omega^{iv})(\varepsilon - \hbar\Omega^{iv})^{1/2}] \qquad (2)$$

with

$$\varepsilon = \begin{cases} E_L - E_{gx}^{i} - \hbar\Omega^{TO(L)} & \text{for } E_L > E_{gx}^{i} + \hbar\Omega^{TO(L)} \\ 0 & \text{for } E_L \leqslant E_{gx}^{i} + \hbar\Omega^{TO(L)} \end{cases}$$

$$C_{iv} = 0 \qquad \text{for } \varepsilon < \hbar\Omega^{iv}.$$

C_0 is the exciton trapping probability at defects and impurities (assumed to be independent on exciton energy). C_{ac} and C_{iv} take into account intravalley long wavelength acoustic and intervalley X-point phonon scattering, respectively. Apart from a nor-

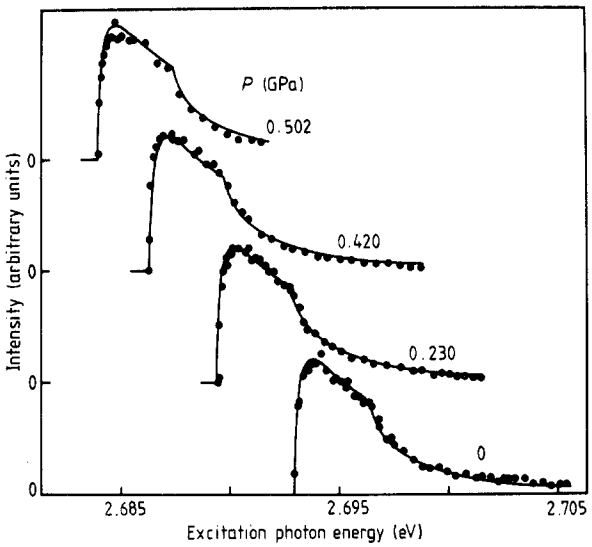

Figure 3. Excitation spectra of the 2TO(L) scattering line in figure 1 at different pressures. The integrated line intensity (full circles) is plotted versus the laser excitation photon energy. The full curves are fits made to the experimental data according to equation (2). All curves are normalised to their maximum intensities.

malisation factor, all experimental data in figure 3 could be fitted by the same set of parameters C_{ac}/C_0 and C_{iv}/C_0 which, within experimental accuracy, agree with those determined earlier from time-resolving measurements (Stolz *et al* 1985). In fitting the data using equation (2), we inserted the pressure-dependent energies of the phonons involved and took into account anti-Stokes as well as Stokes processes in calculating the temperature-dependent scattering rates for the dispersive LA(Γ) phonons (Fujii *et al* 1983).

In particular, we found the parameters independent of pressure implying that no measurable distortion of the exciton band occurs in the pressure regime investigated. From the onset of the 2TO(L) scattering process the pressure dependence of the indirect exciton absorption threshold is derived as

$$dE^i_{ax}/dP = -14.6 \pm 0.1 \text{ meV GPa}^{-1}.$$

Since the onset of exciton absorption originates from TO(L) phonon assistance, the exciton gap and absorption threshold energies are related by

$$E^i_{gx} = E^i_{ax} - \hbar\Omega^{TO(L)}. \tag{3}$$

Taking into account the pressure shift of the phonon energy (table 1), one obtains a pressure coefficient of the indirect exciton gap of

$$dE^i_{gx}/dP = -15.1 \pm 0.2 \text{ meV GPa}^{-1}.$$

Using the isothermal bulk modulus, the corresponding deformation potential constant derived is

$$D^i_{gx} = \frac{dE^i_{gx}}{d(V/V_0)} = -\frac{dE^i_{gx}}{dP} B_T = 0.68 \pm 0.02 \text{ eV}. \tag{4}$$

The determination of the (exciton) deformation potential constant involves, besides

the measured energy shifts, only the bulk modulus. Since this is known with sufficient accuracy, we consider the magnitude of D^{i}_{gx} as certain. In contrast, from analysing the energy dependence of the scattering rate of excitons at long wavelength acoustic phonons in time-resolved measurements, a value $D^{i}_{gx} = 0.90$ eV for the deformation potential was obtained (Stolz *et al* 1985). We believe that this value is too large—essentially due to the uncertainty in effective-mass parameters (neglect of anisotropy), sound velocity and density that enter the evaluation of D^{i}_{gx} in the case of the time-dependent measurements.

It has to be noted that D^{i}_{gx} in general is different from the deformation potential constant D^{ac} of the indirect *electronic* band gap. This is because the exciton binding energy may also change under pressure. For Wannier ($n = 1$) excitons, it may be written within the effective-mass approximation as

$$E^{i}_{bx} = (R/\varepsilon_0^2)(\mu^*/m_0) \tag{5}$$

where R denotes the Rydberg energy, ε_0 is the static dielectric constant, and μ^* and m_0 are the reduced effective exciton and free electron masses, respectively. The dominant pressure effect enters through the pressure dependence of ε_0. Using corresponding data (Lowndes 1972), an upper limit of $+2$ meV GPa^{-1} for $T < 77$ K is estimated for dE^{i}_{bx}/dP resulting in D^{ac} being smaller than D^{i}_{gx} by about 90 meV.

3.2. *Pressure effects of bound exciton transitions*

At low temperature, the luminescence spectrum of AgBr contains sharp line structure associated with excitons recombining at two types of impurity, namely at donor-type centres (Cd^{2+}, Pb^{2+} and others to which an electron becomes trapped) and at iso-electronic iodine. These impurities are unintentionally present even in very pure AgBr crystal material and give rise to two distinctly different types of bound exciton states characterised by their energy positions below the free exciton gap, i.e. by different localisation energies. The behaviour under hydrostatic pressure is also different and reveals differences with respect to the mechanism of exciton binding and electron–lattice coupling.

3.2.1. Excitons bound to neutral donors. The donor-bound exciton complexes are of the type (D^0, X) with localisation energies around 6–8 meV and were recently identified as being associated with various divalent metal ions (Sliwczuk and von der Osten 1988). These impurity centres are able to bind an electron to form a neutral donor at which an exciton may be trapped via its electron, thereby completing the first hydrogenic donor shell in the (D^0, X) complex. Also, silver ions (plus a trapped electron) on interstitial lattice positions belong to this category and are able to trap excitons. Recombination of these excitons gives rise to narrow line luminescence involving L-point phonons. As indicated by the pressure shift of these lines and as summarised in figure 4, these states shift under pressure with a negative pressure coefficient completely parallel to the indirect exciton edge ($dE^{i}_{gx}/dP = -15.1$ meV GPa^{-1}). Consistent with the small localisation energies and also with the participation of momentum-conserving L-point phonons, as in the case of free exciton transitions, this suggests that the bound exciton wavefunctions are identical to those of the free exciton that originate from valence and conduction band states at L and Γ, respectively. The behaviour demonstrates that the (D^0, X) states are to be considered effective-mass states and that the small differences

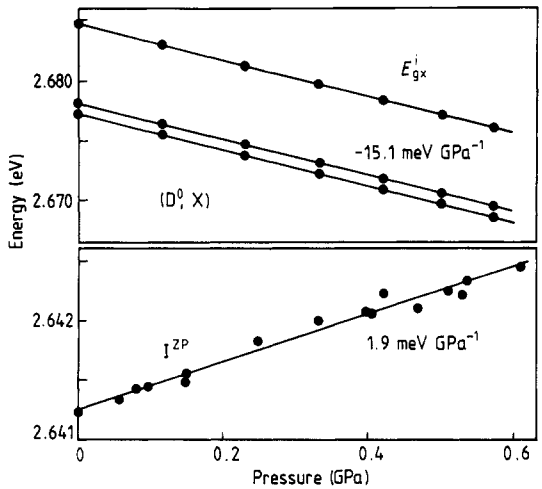

Figure 4. Pressure shift of various free and bound exciton levels in AgBr. E^i_{gx}: indirect free exciton gap energy; (D^0, X): position of donor-bound exciton states derived from the pressure shift of L-point phonon-assisted luminescence lines; I^{ZP}: position of zero-phonon luminescence line of iodine-bound exciton.

in localisation energies (<20% for the ground states) observed for variation of the impurity centres are caused by central cell effects.

3.2.2. The iodine-bound exciton. In this case, isoelectronic iodine in AgBr substitutionally replaces a bromine ion with the exciton bound to the impurity through the hole, essentially because of the difference between the electron affinities of the two halogen atoms. This exciton has been intensely investigated in the past (for references see, e.g., Kanzaki 1986, Czaja and Baldereschi 1979). Its luminescence spectrum is characterised by a zero-phonon line (I^{ZP}) and a strong multiphonon sideband (see figure 5). At low temperature, it exhibits structure due to multiple processes involving LO phonons (Huang–Rhys factor $S \simeq 9$–10), but a detailed analysis has shown that acoustic phonons also interact with appreciable coupling strength and are essential to explain the temperature dependence of the replica intensities (Testa *et al* 1987). From the energetic position of the zero-phonon transition ($E_{ZP} = 2.6412$ eV) with regard to the indirect exciton gap ($E^i_{gx} = 2.6845$ eV), the localisation energy is 43 meV. We have investigated the effect of pressure on both the zero-phonon line and the multiphonon sideband.

Contrasting with the donor-bound exciton states described above, the strong spatial localisation of the hole implies non-vanishing amplitudes of the uppermost valence band wavefunctions from all over the Brillouin zone, especially with some contributions from point Γ as indicated by the appearance of the zero-phonon transition. To investigate these in some more detail, one must take into consideration that, in the present case of relatively strong electron–phonon interaction, besides the electronic states their coupling to the surrounding lattice may also be affected by the pressure. From the configurational coordinate scheme illustrated in figure 6, which presumes, as an approximation, linear electron–lattice coupling, it is straightforward to derive relations

$$E_{LR} = E_{ZP} - E_{max} \tag{6a}$$

$$E_0 = 2E_{ZP} - E_{max} \tag{6b}$$

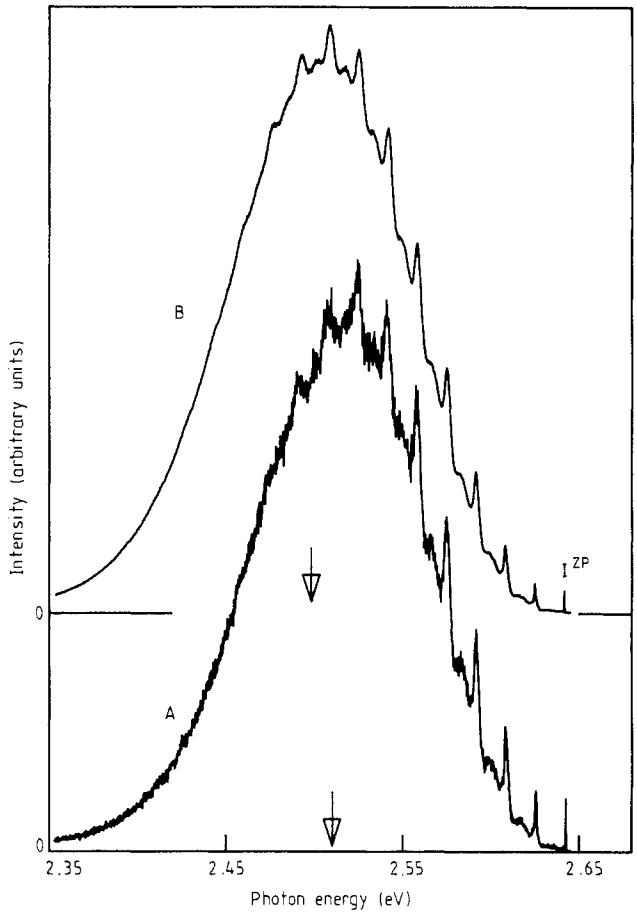

Figure 5. Photoluminescence spectra due to the iodine-bound exciton in nominally pure AgBr at 7 K with and without pressure (A: $P = 0.540$ GPa; B: $P = 0$ GPa). The narrow line structure is due to zero- and multi-LO-phonon processes. The reduction in coupling strength with pressure becomes directly obvious from this structure, which changes in maximum intensity from the $n = 8$ to the $n = 7$ process between spectrum B and A. I^{ZP}: zero-phonon line. Arrows: energy positions of first moment of integrated intensity.

with the quantities defined in the figure. Inserting the measured energies of the zero-phonon transition (E_{ZP}) and of the maximum of the luminescence sideband ($E_{max} = 2.50$ eV) at zero pressure, one obtains the lattice relaxation and bare electronic energies as $E_{LR} = 0.14$ eV and $E_0 = 2.78$ eV, respectively. The pressure shifts observed for the zero-phonon line and for the maximum of the multiphonon sideband imply, through equations (6), that both quantities, E_0 and E_{LR}, are pressure-dependent. With $dE_{ZP}/dP = +1.9$ meV GPa^{-1} (see figure 4) and $dE_{max}/dP = +21.8$ meV GPa^{-1} (measured as the change in first moment of the sideband, see figure 5), one obtains $dE_0/dP = -18.0$ meV GPa^{-1} and $dE_{LR}/dP = -19.9$ meV GPa^{-1} with a linear dependence over the whole pressure range.

The close agreement of dE_0/dP in sign and magnitude with the pressure shift of the indirect exciton gap proves that the iodine-bound exciton state mainly derives from L-point valence band states too. Contributions from Γ that would lead to a positive and

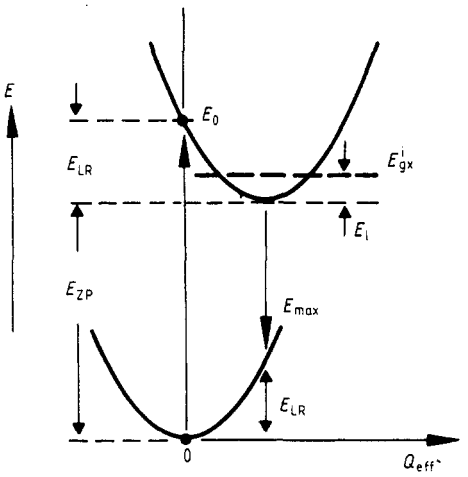

Figure 6. Configurational coordinate model to describe the iodine-bound exciton and to define various energies used in the text. The bound exciton bare electronic energy E_0 is presumed to be situated above the energy E^i_{gx} of the free indirect exciton gap, also indicated.

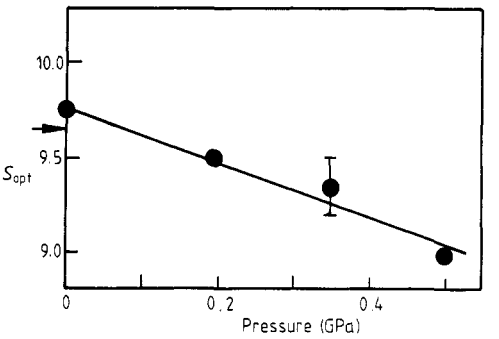

Figure 7. Pressure dependence of the optical phonon coupling constant S_{opt} obtained from the analysis of the low temperature iodine-bound exciton luminescence in figure 5. The arrow at the ordinate marks the zero-pressure value from Czaja and Baldereschi (1979).

much larger shift (pressure shift of direct exciton gap $\mathrm{d}E^{\mathrm{d}}_{gx}/\mathrm{d}P = +63$ meV GPa^{-1} (Aust 1968)) are evidently only small. Although the linear coupling assumed to analyse the pressure data is only a first approximation and certainly does not take full account of the electron–lattice interaction, the result obtained is consistent with other observations. In particular, it explains the relatively long lifetime of 18 μs measured for the iodine-bound exciton (Kanzaki and Sakuragi 1969) indicating the still indirect character of this transition. As was discussed previously (Czaja and Baldereschi 1979), contributions from the uppermost valence band at Γ are indeed expected to be weak since they are weighted by an energy denominator of about 2 eV compared with the much smaller binding energy involved.

Regarding the iodine-bound exciton ground state, the difference in pressure coefficients of the indirect exciton gap and the zero-phonon line (E^i_{gx} and I^{ZP} in figure 4) demonstrates a decrease in localisation energy with increasing pressure. An extrapolation in figure 4 shows that it will become unstable relative to the free exciton at about $P = 3.3$ GPa. Recent experiments in mixed silver halides $AgBr_{0.85}Cl_{0.15}$ under much larger hydrostatic pressure (Kobayashi *et al* 1983, Yokoyama and Kobayashi 1985) showed that the luminescence due to the iodine-bound exciton vanishes at $P = 3.2$ GPa in very good agreement with our results in pure AgBr.

Within the linear electron–phonon coupling model represented by the configurational coordinate diagram in figure 6, the lattice relaxation energy is given by

$$E^{\mathrm{opt}}_{\mathrm{LR}} = S_{\mathrm{opt}}\hbar\Omega^{\mathrm{LO}} \tag{7}$$

where we restrict ourselves to coupling to optical phonons taking $\hbar\Omega^{\mathrm{LO}}$ as the (average) phonon energy and S_{opt} as the Huang–Rhys coupling strength. Equation (7) implies that

the observed pressure-induced change in lattice relaxation energy may originate from changes in both of these quantities as formally expressed by the pressure derivative

$$dE_{LR}^{opt}/dP = (dS_{opt}/dP)\hbar\Omega^{LO} + S_{opt}\, d(\hbar\Omega^{LO})/dP. \tag{8}$$

The appearance of discrete optical phonon structure in the luminescence band (cf figure 5) enabled us to perform a detailed analysis that provides each of the quantities on the right-hand side of equation (8) and allows us to determine the two contributions to dE_{LR}^{opt}/dP separately. To obtain the optical phonon part to the total sideband intensity, we employed the procedure previously proposed and applied by Czaja and Baldereschi (1979). We subtracted the (smooth) spectrum measured at some higher temperature ($T \simeq 20$ K)—supposed to be mainly due to acoustic phonon coupling—from the low temperature (7 K) spectrum in figure 5 containing intensity from acoustic and optic phonon interactions. Analysing the remaining LO phonon sideband (thereby assuming for the nth phonon contribution a lorentzian with linewidtdh $\Gamma_n = n\Gamma_1$ proportional to the phonon number) from the expected Poisson distribution of intensities, average values of the coupling strength S_{opt} were determined for different pressures. The result of this analysis is summarised in figure 7. It shows a clear reduction in coupling strength from its zero-pressure value $S_{opt} = 9.75$ with $dS_{opt}/dP = -1.5$ GPa^{-1} that corresponds to an 8% change in S_{opt} at the maximum pressure of 0.5 GPa (see figure 5). The phonon energy and pressure coefficient following from the spectra are $\hbar\Omega^{LO} = 16.6$ meV and $d(\hbar\Omega^{LO})/dP = +0.45$ meV GPa^{-1}, whereby these numbers represent average values. As already recognised earlier for the LO phonon energy (Czaja and Baldereschi 1979), a systematic dependence on phonon number n is found for these quantities. Evaluating equation (8), we obtain

$$dE_{LR}^{opt}/dP = -24.9 + 4.4 \text{ meV GPa}^{-1} = -20.5 \text{ meV GPa}^{-1}$$

which shows that the pressure-induced change in lattice relaxation energy is to a large extent caused by the changing electron–phonon coupling strength, which is compensated only slightly by the effect due to the change in phonon energy. Comparison of dE_{LR}^{opt}/dP with the corresponding value for the combined acoustic and optical phonon sideband (-19.9 meV GPa^{-1}) derived above from equations (6) shows good agreement and confirms nicely the consistency of the analysis.

4. Concluding remarks

Comparing the donor- and the iodine-bound exciton states, the analysis of their luminescence transitions under hydrostatic pressure proves that both derive from L-point valence band states with only minor Γ contributions that produce the weak zero-phonon line in the case of the iodine-bound exciton. At first sight, this is surprising since the binding energies of the two excitons are markedly different (6–8 meV and 43 meV, respectively) and the (D^0, X) recombination luminescence and the iodine-bound exciton zero-phonon line (I^{ZP}) exhibit quite different pressure shifts (cf figure 4). It is the lattice relaxation that occurs in the case of the iodine-bound exciton and that is connected with the mechanism of exciton binding (the exciton is bound through the hole to the isoelectronic impurity) that finally gives rise to the observed differences. Since no relaxation is involved in the case of the donor-bound excitons (binding through the electron filling up a hydrogen-like 1s shell), the optical transitions involving L-point

states entirely parallel the negative pressure shift of the indirect free exciton state at E_{gx}^{i}.

We finally mention that both $\hbar\Omega^{LO}$ and $d(\hbar\Omega^{LO})/dP$ determined from the iodine-bound exciton luminescence are distinctly different in magnitude from the corresponding LO phonon values obtained from the resonant Raman data for the free exciton (cf table 1). We believe that the reason for this is that in the case of the bound exciton state a local rather than an extended phonon mode interacts. The observed reduction in phonon energy with regard to the unperturbed lattice is qualitatively consistent with the larger mass of the iodine ion replacing a bromine ion in AgBr.

Acknowledgments

We thank Professor W B Holzapfel for his support in developing the pressure technique and Dr H Hochheimer for temporarily lending us a high pressure cell at the beginning of this study.

References

Aust R B 1968 *Phys. Rev.* **170** 784
Brothers A D and Lynch D W 1969 *Phys. Rev.* **180** 911
Czaja W and Baldereschi A 1979 *J. Phys. C: Solid State Phys.* **12** 405
Dugdale J S 1958 *Nuovo Cimento* **9** Suppl. 27
Fitchen D B 1963 *Rev. Sci. Instrum.* **34** 673
Fujii A, Stolz H and von der Osten W 1983 *J. Phys. C: Solid State Phys.* **16** 1713
Kanzaki H 1986 *Excitonic Processes in Solids (Springer Series in Solid-State Sciences* 60) ed M Cardona, P Fulde, K von Klitzing, H J Queisser (Berlin: Springer)
Kanzaki H and Sakuragi S 1969 *J. Phys. Soc. Japan* **27** 109
Kobayashi M, Kawamura T, Endo S, Cho K and Narita S 1983 *Solid State Commun.* **9** 999
Lowndes R P 1972 *Phys. Rev.* B **6** 4667
Marklund K, Vallin J and Mahmoud S A 1969 *Uppsala University Institute of Physics Report No* UUIP-645
Schock R N and Jamieson J C 1969 *J. Phys. Chem. Solids* **30** 1527
Sliwczuk U, Stolz H and von der Osten W 1984 *Phys. Status Solidi* b **122** 203
Sliwczuk U and von der Osten W 1988 *J. Imaging Sci.* **32** 106
Slykhouse T E and Drickamer H G 1958 *J. Phys. Chem. Solids* **7** 207
Stolz H, Schreiber E and von der Osten W 1985 *Proc. 17th Int. Conf. Physics of Semiconductors (San Francisco)* ed J D Chadi and W A Harrison (New York: Springer) p 1271
Testa A, Czaja W, Quattropani A and Schwendimann P 1987 *J. Phys. C: Solid State Phys.* **20** 1253
von der Osten W 1984 *NATO ASI Series B: Physics* vol 108, ed J T Devreese and F Peeters (New York: Plenum) p 293
Windscheif J and von der Osten W 1980 *J. Phys. C: Solid State Phys.* **13** 6299
Yokoyama T and Kobayashi M 1985 *J. Phys. Soc. Japan* **54** 2329